Transformation of subradiant states to superradiant states in a thick resonant medium

R. N. Shakhmuratov

Kazan Physical-Technical Institute, Russian Academy of Sciences, 10/7 Sibirsky Trakt, Kazan 420029, Russia and Kazan Federal University, 18 Kremlyovskaya Street, Kazan 420008, Russia

(Received 5 December 2013; published 15 July 2014)

The propagation of a step pulse through a thick resonant absorber with a homogeneously broadened absorption line is considered. It is shown that a specific subradiant state is naturally developed in the absorber due to the formation of the spatial domains of the atomic coherence with opposite phases. It is proposed to divide the absorber into slices in accordance with these domains and place the phase shifters in front of the first slice and between the other slices. If the phase shifters are switched on simultaneously at a particular moment of time, elapsed from the beginning of the step pulse, a strong sharp pulse is generated at the output of the last slice of the absorber. The effect is explained by the phasing of the atomic coherence along all slices of the absorber, which transforms the subradiant state of the atom-field system to a superradiant state.

DOI: 10.1103/PhysRevA.90.013819 PACS number(s): 42.50.Gy, 42.25.Bs, 42.50.Nn

I. INTRODUCTION

The resonant interaction of a weak coherent pulse with extended dielectric absorbers in a linear regime is well described by the exact integral representation of the propagating plane-wave field if the spectrum of the input pulse and the complex dielectric permittivity of the medium are known (see, for example, Refs. [1,2]). This integral is quite simple and can be easily calculated numerically. Meanwhile, sometimes it is not obvious how to calculate the output field if we modify the field or the induced polarization inside the medium during the pulse propagation. In this case, knowledge of the Green's function of the dispersive dielectric medium (its response to a δ-function input pulse) helps to find the shape of the output pulse (see, for example, Ref. [3]).

Change of the field phase or change of the induced polarization in the medium along the pulse propagation are quite effective methods of creating subradiant and superradiant states. Transferring the radiation field between these states was proposed in a sequence of papers (see Refs. [4–8]) to create a quantum memory for single photons. In these papers such a transformation was intended to implement, by coherent pulses, exciting atoms on auxiliary transitions (adjacent to a resonant one), by a particular variant of the CRIB technique (controlled reversible inhomogeneous broadening) or by controllable phase modulators of the field (phase shifters), inserted into the atomic ensemble in a regular way along the direction of the signal pulse propagation. All these methods imply an artificial creation of periodic spatial domains from atomic dipoles, induced by the input signal field, such that dipoles in neighboring domains have opposite phases. This operation produces a locked atom-field subradiant state. It is a storage stage in a quantum memory protocol. In a reading stage all domains of polarization are brought in phase, which results in the superradiance, i.e., fast release of the radiation field.

In this paper it is found that a step (or rectangular) pulse propagating in an optically thick resonant medium creates such domains of polarization with opposite phases naturally. Their lengths are not equal and evolve in time. Thus we may take for granted a naturally built-up atom-field subradiant state. It is proposed to cut the sample into unequal slices in a particular way and place phase shifters between them. Then at a given moment of time their fast switch on results in the superradiance, seen as a short and strong pulse.

II. SPATIAL OSCILLATIONS OF THE ATOMIC POLARIZATION ALONG THE LIGHT BEAM IN A THICK RESONANT MEDIUM

For simplicity, we consider the propagation of a weak pulse in a thick resonant medium with a homogeneously broadened absorption line. A generalization to the case of inhomogeneously broadened absorption line with Lorentzian shape is trivial (see, for example, Ref. [1]).

In the slowly varying amplitude (SVA) approximation, the unidirectional propagation of a weak pulse $E(z,t)$ as a plane wave along axis $\mathbf{z}$ is described by a couple of the atom-field equations appropriate for the linear response (LR) approximation. These equations are

$$\dot{\sigma}_{eg} = -\gamma\sigma_{eg} + i\Omega(z,t), \tag{1}$$

$$\widehat{L}\Omega(z,t) = i\alpha\gamma\sigma_{eg}(z,t)/2, \tag{2}$$

where $\rho_{eg} = \sigma_{eg}\exp(-i\omega t + ikz)$ is the nondiagonal element of the atomic density matrix and σ_{eg} its slowly varying part; ω and k are the frequency and wave number of the pulse propagating along axis $\mathbf{z}$ (here z is a coordinate along $\mathbf{z}$); γ is the decay rate of the atomic coherence; $\Omega(z,t) = d_{eg}E_0(z,t)/2\hbar$, where d_{eg} is a matrix element of the dipole transition between ground g and excited e states of an atom; $E_0(z,t) = E(z,t)\exp(i\omega t - ikz)$ is a slowly varying field amplitude; $\widehat{L} = \partial_z + c^{-1}d_t$; and α is the resonant absorption coefficient. We limit our consideration to the case of exact resonance.

These equations are easily solved by means of the Fourier transform,

$$F(\nu) = \int_{-\infty}^{+\infty} f(t)e^{i\nu t}dt, \tag{3}$$

which reduces them to a couple of algebraic equations,

$$\sigma_{\rm eg}(z,\nu) = -\frac{\Omega(z,\nu)}{\nu + i\gamma}, \tag{4}$$

$$\left[\frac{\partial}{\partial z} - \frac{i\nu}{c} + A(\nu)\right]\Omega(z,\nu) = 0, \tag{5}$$

where

$$A(\nu) = \frac{i\alpha\gamma/2}{\nu + i\gamma}. \tag{6}$$

The solution is

$$\Omega(z,\nu) = \Omega(0,\nu)\exp\left[(i\nu z/c) - A(\nu)z\right], \tag{7}$$

where $\Omega(0,\nu)$ is the Fourier transform of the input field envelope at the front face of the absorber with coordinate $z = 0$. The inverse Fourier transform of Eq. (7) gives the familiar expression for the development of the radiation field in the resonant absorber with distance, that is,

$$\Omega(z,t) = \frac{1}{2\pi}\int_{-\infty}^{+\infty}\Omega(0,\nu)\exp\left[-i\nu(t - z/c) - A(\nu)z\right]. \tag{8}$$

Below, for simplicity of notation, we disregard the small value z/c.

For the input step pulse, $\Omega_\Theta(0,t) = \Omega_0\Theta(t)$, which is switched on at $t = 0$ and has the amplitude Ω_0 [here $\Theta(t)$ is the Heaviside step function], the integral in the solution (8) was calculated in Ref. [1]. The result is expressed in terms of infinite sum of the Bessel functions of ascending order, multiplied by the coefficients, depending on α, γ, and t. To simplify calculation of the integral in Eq. (8), it is usually reduced with the help of the convolution theorem to (see, for example, Refs. [9–11])

$$\Omega(z,t) = \int_{-\infty}^{+\infty}\Omega(0,t-\tau)R(z,\tau)d\tau, \tag{9}$$

where $R(z,\tau)$ is the output radiation from the absorber of length z, if the input radiation is a very short pulse whose shape is described by the Dirac δ function $\delta(t)$, i.e., $R(z,\tau)$ is the Green's function of the absorber of thickness z. This function is [1,9,10,12]

$$R(z,t) = \delta(t) - e^{-\gamma t}\Theta(t)\sqrt{\frac{b}{t}}J_1(2\sqrt{bt}), \tag{10}$$

where $J_1(x)$ is the first-order Bessel function, $b = \alpha z\gamma/2$, and t is the local time, defined in the retarded reference frame as $t_r = t - z/c$. Below we drop the index r; however, we keep in mind that this time depends on z. The inverse value of b is referred to as superradiant time $T_R = 1/b$ (see Ref. [8]). Then the parameter b may be referred to as superradiant rate. It is also referred to as the effective thickness parameter, since for the absorber of thickness z this parameter is proportional to z.

For the input step pulse equation (9) is reduced to (see, for example, Refs. [9,13])

$$\Omega_\Theta(z,t) = \Omega_0\Theta(t)\left[e^{-\gamma t}J_0(2\sqrt{bt}) + \gamma\int_0^t e^{-\gamma\tau}J_0(2\sqrt{b\tau})d\tau\right]. \tag{11}$$

Another version of this expression,

$$\Omega_\Theta(z,t) = \Omega_0\Theta(t)\left[1 - \int_0^t e^{-\gamma\tau}\sqrt{\frac{b}{\tau}}J_1(2\sqrt{b\tau})d\tau\right], \tag{12}$$

can be found, for example, in Refs. [10,11]). Meanwhile, the equation for the output field can be expressed in a fast converging series (see Appendix in Ref. [13]),

$$\Omega_\Theta(z,t) = \Omega_0\Theta(t)\left\{e^{-b/\gamma} + e^{-\gamma t}\left[f_0(b)J_0(2\sqrt{bt}) + \sum_{n=1}^{\infty}f_n(b,t)j_n(bt)\right]\right\}, \tag{13}$$

where $j_n(bt) = J_n(2\sqrt{bt})/(bt)^{n/2}$, $J_n(2\sqrt{bt})$ is the Bessel function of the nth order, $f_0(b) = f_0(b,t) = 1 - \exp(-b/\gamma)$, and

$$f_n(b,t) = (\gamma t)^n\left[1 - e^{-b/\gamma}\sum_{k=0}^{n}\frac{(b/\gamma)^k}{k!}\right]. \tag{14}$$

It should be noted that the sum in Eq. (14) is a truncated Taylor series for $\exp(b/\gamma)$. Thus, with increase of n, the expression in square brackets in Eq. (14) tends to zero, i.e.,

$$\lim_{n\to\infty}\left[1 - e^{-b/\gamma}\sum_{k=0}^{n}\frac{(b/\gamma)^k}{k!}\right] = 0. \tag{15}$$

Depending on the values of the parameters b and γ, it is enough to take into account only one or two first terms in the sum, which is the third term in Eq. (13), to obtain a fine approximation for $\Omega_\Theta(z,t)$. If $b \gg \gamma$, i.e., the superradiant rate is much faster than the decay rate of the atomic coherence, then time evolution of the output field $\Omega_\Theta(z,t)$ is well approximated by the function

$$\Omega_\Theta(z,t) \approx \Omega_0\Theta(t)e^{-\gamma t}J_0(2\sqrt{bt}), \tag{16}$$

which is the main part of the second term in Eq. (13). Other terms give minor contribution. This condition is satisfied if $\alpha l/2 \gg 1$, where l is the length of the absorbing sample.

To find the spatiotemporal evolution of the atomic coherence along the sample we can use Eq. (4) and obtain, according to the convolution theorem, the result

$$\sigma_{\rm eg}(z,t) = i\int_{-\infty}^{+\infty}e^{-\gamma(t-\tau)}\Theta(t-\tau)\Omega(z,\tau)d\tau, \tag{17}$$

where z changes between 0, which is a coordinate of the front face of the sample, and l, which is a coordinate of the sample end. For the step pulse Eq. (17) is reduced to (see Ref. [13])

$$\sigma_{\rm eg}(z,t) = i\Omega_0\Theta(t)\int_0^t e^{-\gamma\tau}J_0(2\sqrt{b\tau})d\tau. \tag{18}$$

From Eqs. (11) and (13) it follows that the atomic coherence can be expressed as

$$\sigma_{\rm eg}(z,t) = \frac{i\Omega_0}{\gamma}\Theta(t)\left\{e^{-\gamma t}\sum_{n=1}^{\infty}f_n(b,t)j_n(bt) + e^{-b/\gamma}\left[1 - e^{-\gamma t}J_0(2\sqrt{bt})\right]\right\}. \tag{19}$$

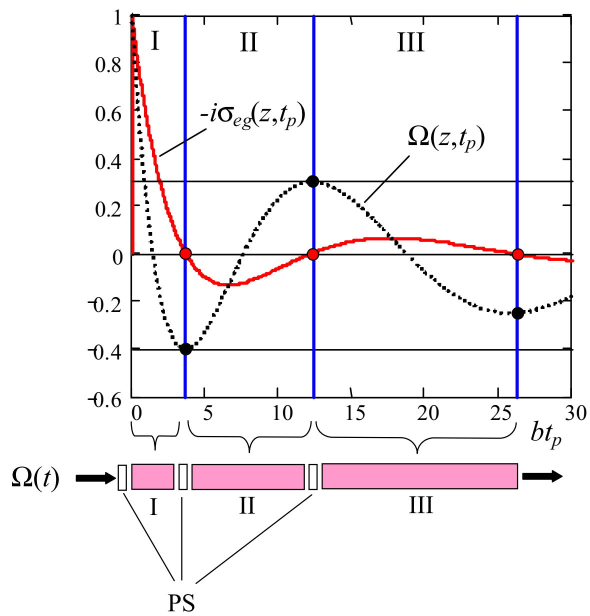

FIG. 1. (Color online) Spatial dependencies of the imaginary part of the atomic coherence, $-i\sigma_{\mathrm{eg}}(z,t_p)$, (solid line in red) and the radiation field, $\Omega(z,t_p)$, (dotted black line) along the absorber at $t = t_p$. Both are normalized to 1 (see the text for details). Vertical bold blue lines divide the plot into domains (I, II, and III), where the imaginary part of the atomic coherence has one sign (plus or minus). Thin horizontal lines show the values of the two first extrema of the field amplitude. The excitation scheme of the absorber, cut into slices, and phase shifters (PSs) placed between them, are shown in the bottom.

If $b \gg \gamma$, then evolution of the atomic coherence is well approximated by the main part of the first term in the sum in Eq. (19), which is

$$\sigma_{\mathrm{eg}}(z,t) \approx i\Omega_0 t\Theta(t)e^{-\gamma t}\frac{J_1(2\sqrt{bt})}{\sqrt{bt}}. \tag{20}$$

The coherence $\sigma_{\mathrm{eg}}(z,t)$ is purely imaginary, since the radiation field is in exact resonance. The sign of this coherence oscillates with time t and distance z (since $b = \alpha z\gamma/2$) according to the Bessel function $J_1(2\sqrt{bt})$.

We choose time t_p satisfying the condition $b_l t_p \gg 1$, where $b_l = \alpha l\gamma/2$ and l is the coordinate of the output facet of the sample. Spatial dependencies of the radiation field $\Omega_\Theta(z,t_p)$ (dotted line) and the imaginary part of the coherence $\sigma_{\mathrm{eg}}(z,t_p)$ (solid line) along the sample, if $\gamma t_p \to 0$ and $b_l t_p = 30$, are shown in Fig. 1. In this case $\Omega_\Theta(z,t_p)$ and $\sigma_{\mathrm{eg}}(z,t_p)$ are well described by Eqs. (16) and (20), respectively. The plot of the field amplitude is normalized to Ω_0 and the atomic coherence to $\Omega_0 t_p$; thus both are defined as nondimensional values, which have the same maxima equal to 1.

In one's mind the sample can be divided into several domains such that in the neighboring domains the atomic coherences have opposite phases. This phenomenon can be understood with the help of the concept of Feynman *et al.* [14], explaining how the light propagates in a linear regime through a dielectric medium.

According to his concept, the radiation field at the output of a finite-size sample can be considered as a result of the interference of the input field, as if it would propagate without interaction, with the secondary field radiated by the linear polarization induced in the sample. The secondary field is actually a coherently scattered field whose phase is opposite to the phase of the incident radiation field. Destructive interference of these fields leads to attenuation of the radiation field at the output of the sample.

In Fig. 1 the sample is divided into three domains marked by vertical lines, placed at coordinates z (in units of bt_p), where $\sigma_{\mathrm{eg}}(z,t_p)$ is zero. Below we refer to the coordinates of the right borders of the domains I, II, and III as z_1, z_2, and z_3, respectively.

In domain I the imaginary part of the atomic coherence is positive. Therefore the phase of the coherently scattered field is opposite to the phase of the incident field, and the sum of these fields, $\Omega(z,t_p)$, is attenuated due to their destructive interference. As a result, the sum field and atomic coherence decrease with distance.

At some distance the sum field, $\Omega(z,t_p)$, becomes zero. However, this process has some inertia due to the energy accumulation in the atomic excitation. Therefore, at a particular distance the scattered field becomes even greater than the incident field, producing the phase change of the sum field, $\Omega(z,t_p)$. This is also confirmed by the wave equation (2), rewritten in the retarded reference frame as

$$\partial\Omega(z,t_r)/\partial z = i\alpha\gamma\sigma_{\mathrm{eg}}(z,t_r)/2. \tag{21}$$

From this equation it is seen that if the imaginary part of $\sigma_{\mathrm{eg}}(z,t_r)$ is positive, the spatial derivative of the sum field is negative and this derivative becomes zero only if $\sigma_{\mathrm{eg}}(z,t_r) = 0$, which takes place at coordinate z_1. Thus, before coordinate z_1 the atomic coherence forces the sum field $\Omega(z,t_p)$ to decrease, and when the sum field becomes zero the atomic coherence continues this tendency, making the field amplitude negative.

After the point where the sum field becomes negative, the field in its turn tends to reverse the phase of the coherence, bringing its amplitude to zero at z_1 [marked by the first gray (red) circle on the left in Fig. 1]. This process is oscillatory and is repeated in the next domains.

According to Eqs. (16) and (20) [as well as Eq. (21)], the absolute value of the sum field $\Omega(z,t_p)$ reaches its local maxima at coordinates where $\sigma_{\mathrm{eg}}(z,t_p) = 0$. Since at these points the amplitude of the coherently scattered field takes maximum values, we propose to shift the phase of the sum fields simultaneously at the same points by π, including the front face of the sample. Then we expect that in all domains the incident and scattered fields will interfere constructively, producing a pulse of large amplitude. The position of the phase shifters (PS) in the sample, cut into slices at coordinates z_1, z_2, and z_3, is shown at the bottom of Fig. 1. Effectively, such a phase shift of the sum fields will force the atomic coherences to amplify the field along the whole sample coherently, i.e., we will cause effective phasing of the atomic coherences in all domains shown in Fig. 1. The phases of the atomic coherences in each domain will be $-\pi/2$ with respect to the fields incident to the domain.

III. DOMAIN I

Assume that at time $t_p > 0$ the value of the coherence of the particles, located at the output facet of the sample, reaches its first zero value, $\sigma_{eg}(l,t_p) = 0$. This condition is satisfied if $b_l t_p = 3.67$. By that time only domain I of atomic coherence (see Fig. 1) is developed in the sample. At the same time we instantly change the phase of the input field by π. Then the incident field becomes in phase with the secondary (coherently scattered) field. Their constructive interference should result in a strong and short pulse.

To find the transients, induced by that phase shift, we consider the incident radiation field $\Omega(0,t)$ as consisting of two pulses, i.e.,

$$\Omega_1(0,t) = \Omega_\Theta(0,t) - 2\Omega_\Theta(0,t - t_p), \quad (22)$$

where $\Omega_\Theta(0,t) = \Omega_0\Theta(t)$ is the step pulse, defined in the previous section. Then the output field is

$$\Omega_1(z_1,t) = \Omega_\Theta(z_1,t) - 2\Omega_\Theta(z_1,t - t_p). \quad (23)$$

Here the function $\Omega_\Theta(z_1,\tau)$ is defined in Eqs. (11) and (13), where $b = b_1 = \alpha z_1\gamma/2$ and $z_1 = l$. If $b_1 \gg \gamma$, the approximate equation (16) is valid, and then

$$\Omega_1(z_1,t) = \Omega_0[\Theta(t)e^{-\gamma t}J_0(2\sqrt{b_1 t}) - 2\Theta(t - t_p)e^{-\gamma(t-t_p)} \times J_0(2\sqrt{b_1(t - t_p)})]. \quad (24)$$

From this equation we see that just after t_p ($t = t_p + 0$) the amplitude of the output field is

$$\Omega_1(z_1,t_p) = \Omega_0[e^{-\gamma t_p}J_0(2\sqrt{b_1 t_p}) - 2]. \quad (25)$$

If $\gamma t_p \ll 1$, then the maximum amplitude of the pulse is $\Omega_1(z_1,t_p) = -2.4\Omega_0$, its phase is opposite to the phase of the input field, and intensity is 5.76 times larger than the intensity of the incident radiation field. The shape of the pulse is shown in Fig. 2, where the intensity of the output field is plotted without approximation (16) for different values of the decay rate of the atomic coherence γ.

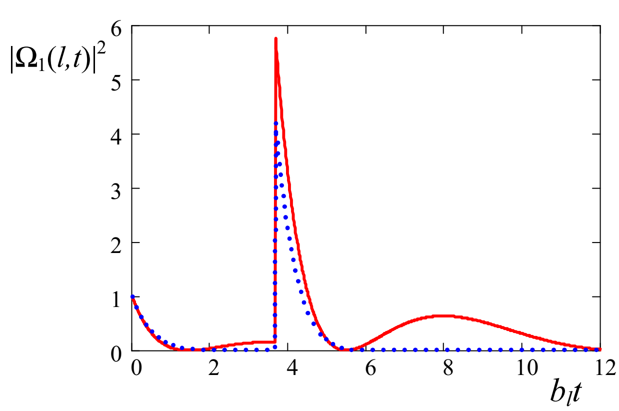

FIG. 2. (Color online) The field intensity and the shape of the pulse, generated at the output of the sample by the phase shift of the radiation field, applied at the input at time t_p satisfying the condition $b_l t_p = 3.67$. b_l is the superradiant parameter of the sample. The field intensity is normalized to $|\Omega_0|^2$. The decay rates of the atomic coherence are $\gamma = 0.003 b_l$ (solid line in red) and $\gamma = 0.3 b_l$ (dotted line in blue).

IV. DOMAINS I PLUS II

In this section we consider the case if $b_l t_p = 12.3$. Then, by time t_p two domains (I and II, see Fig. 1) are developed in the absorber. We could cut the absorber of length l into two slices of lengths z_1 and $l - z_1$, where z_1 satisfies the relation $\alpha z_1 \gamma t_p/2 = 3.67$. Below we define the parameters b_1 and b_2 for these slices, which are $b_1 = 3.67/t_p$ and $b_2 = 8.63/t_p$. Then, by definition, we have $b_1 + b_2 = b_l$. We can make a gap δ_{12} between these slices and place the phase shifters in front of each slice (see the bottom of Fig. 1). When phase shifters are off, the input and hence output fields for the second slice acquire an additional phase factor $\exp(ik\delta_{12})$ due to the gap between slices. The distance between the slices can be quite large to be able to place the phase shifter not touching the absorbing slices. We assume that within the gap, where there is no absorbing medium, the amplitude of the field does not change and only its phase φ changes to $\varphi + ik\delta_{12}$. Therefore, in the second slice the evolution of the field and the atomic polarization is identical to that shown in Fig. 1, where this gap is zero ($\delta_{12} = 0$), except for the total phase shift, $ik\delta_{12}$, of both the field and polarization. Below we neglect this phase factor, since it does not affect the intensity of the output field from the composite absorber.

The output field from the first slice of the composite absorber, $\Omega_1(z_1,t)$, is described by Eq. (23), where the cooperative rate b is b_1. Due to the second phase shifter, switched on at t_p (see Fig. 1), the input field for the second slice is $\Omega_1(z_1,t)[1 - 2\Theta(t - t_p)]$. The explicit expression for this field is

$$\Omega_{\pi 1}(z_1,t) = \Omega_\Theta(z_1,t)[1 - 2\Theta(t - t_p)] + 2\Omega_\Theta(z_1,t - t_p), \quad (26)$$

where the index π means that the phase of the field $\Omega_1(z_1,t)$ is changed by π. Here we disregard the distance δ_{12} between pieces and put its value equal to zero, since its contribution to the intensity of the output field from the composite absorber is zero for any value of δ_{12}.

With the help of Eq. (9), one can calculate the radiation field $\Omega_2(z_2,t)$ at the output of the second slice and obtain the expression, which is reduced to

$$\Omega_2(z_2,t) = \Omega_\Theta(z_2,t) + 2\Omega_\Theta(z_2,t - t_p) - 2\Theta(t - t_p)\Omega_{12}(z_1,z_2,t,t_p). \quad (27)$$

Here the functions $\Omega_\Theta(z_2,t)$ and $\Omega_\Theta(z_2,t - t_p)$ are defined in Eq. (11), where the superradiant rate b is substituted by the sum of the superradiant rates of the slices, i.e., $b_l = b_1 + b_2$, the gap between slices δ_{12} being omitted. These functions describe those components of the output field from the second slice, which are produced by the input fields $\Omega_\Theta(z_1,t)$ and $\Omega_\Theta(z_1,t - t_p)$, respectively. Their derivation is given in the Appendix. The function $\Omega_{12}(z_1,z_2,t,t_p)$ (valid for $t \geq t_p$) is

$$\Omega_{12}(z_1,z_2,t,t_p) = \Omega_\Theta(z_1,t) - b_2 \times \int_0^{t-t_p} \Omega_\Theta(z_1,t - \tau)e^{-\gamma\tau} j_1(b_2\tau)d\tau. \quad (28)$$

It describes the transformation of the field $\Theta(t - t_p)\Omega_\Theta(z_1,t)$ by the second slice of the absorber. The function $j_1(b_2\tau)$ is defined just after Eq. (13). Multiple integration in Eq. (28) can

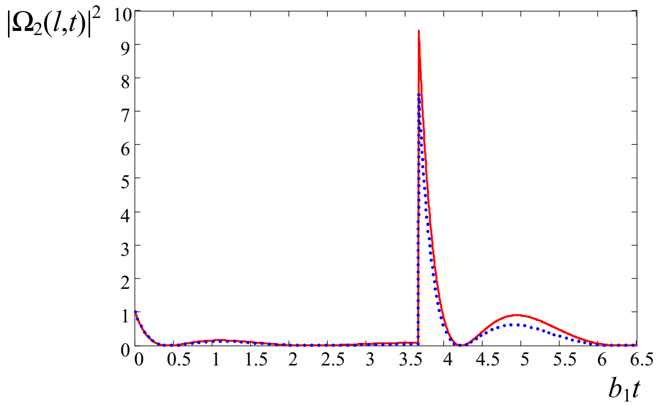

FIG. 3. (Color online) The field intensity at the output of the composite absorber consisting of two slices. The π-phase shift of the fields at the input of the first and second slices of the composite absorber are applied at time t_p satisfying the condition $b_1 t_p = 3.67$, where b_1 is the superradiant rate of the first slice. The time scale is normalized to this rate. The field intensity is normalized to $|\Omega_0|^2$. The decay rates of the atomic coherence are $\gamma = 0.01 b_1$ (solid line in red) and $\gamma = 0.1 b_1$ (dotted line in blue).

be avoided if instead of Eq. (11) for $\Omega_\Theta(z_1, t-\tau)$ one uses Eq. (13).

Just after the phase shift of the fields (at time $t = t_p + 0$), the amplitude of the output field from the second slice is

$$\Omega_2(z_2,t_p) = \Omega_\Theta(z_2,t_p) + 2\Omega_\Theta(z_2,0) - 2\Omega_\Theta(z_1,t_p). \tag{29}$$

If $b_{1,2} \gg \gamma$, then according to the approximate equation (16), this amplitude is approximated as

$$\Omega_2(z_2,t_p) = \Omega_0\{2 + e^{-\gamma t_p}[J_0(2\sqrt{(b_1+b_2)t_p}) - 2J_0(2\sqrt{b_1 t_p})]\}. \tag{30}$$

If $\gamma t_p \ll 1$, then for the chosen values of the superradiant rates of the slices, i.e., $b_1 = 3.67/t_p$ and $b_2 = 8.63/t_p$, the amplitude of the output field is $3.1\Omega_0$ and its intensity is 9.65 times larger than the intensity of the incident radiation field. The shape of the pulse appearing at the output of the composite absorber after the phase shift of the fields is shown in Fig. 3, where the output field intensity is plotted according to Eq. (27) for different values of the decay rate of the atomic coherence γ.

V. THREE DOMAINS

If by time t_p the superradiant rate of the absorber b_l satisfies the relation $b_l t_p = 25.87$, then three domains are developed inside the absorber. We divide such absorber in three slices satisfying the relations $b_1 t_p = 3.67$, $b_2 t_p = 8.63$, and $b_3 t_p = 13.57$, where $b_k = \alpha l_k \gamma/2$, and l_k is the thickness of the kth slice, which is related to the coordinates z_k of the domain borders (see Fig. 1) as follows: $l_1 = z_1$, $l_2 = z_2 - z_1$, and $l_3 = z_3 - z_2$. We make gaps between the slices and place phase shifters between them and before the first slice.

In the previous section it was shown that after the π-phase shift of the fields before the first and second slices, the output field from the second slice $\Omega_2(z_2,t)$ is described by Eq. (27). Due to its π-phase shift, produced between the second and third slices by the phase shifter, the input field for the third slice is

$$\Omega_{\pi 2}(z_2,t) = \Omega_\Theta(z_2,t)[1 - 2\Theta(t-t_p)] - 2\Omega_\Theta(z_2,t-t_p) + 2\Theta(t-t_p)\Omega_{12}(z_1,z_2,t,t_p). \tag{31}$$

With the help of Eq. (9), we calculate the amplitude of the radiation field $\Omega_3(z_3,t)$ at the output of the third slice, which is

$$\Omega(z_3,t) = \Omega_\Theta(z_3,t) + 2\Theta(t-t_p)[A(t) + B(t) + C(t) + D(t)], \tag{32}$$

where

$$A(t) = \Omega_\Theta(z_1,t) - \Omega_\Theta(z_2,t) - \Omega_\Theta(z_3,t-t_p), \tag{33}$$

$$B(t) = -b_2 \int_0^{t-t_d} \Omega_\Theta(z_1,t-\tau) e^{-\gamma\tau} j_1(b_2\tau) d\tau, \tag{34}$$

$$C(t) = -b_3 \int_0^{t-t_d} [\Omega_\Theta(z_1,t-\tau) - \Omega_\Theta(z_2,t-\tau)] e^{-\gamma\tau} \times j_1(b_3\tau) d\tau, \tag{35}$$

$$D(t) = b_2 b_3 \int_0^{t-t_d} d\tau_1 \int_0^{t-t_d-\tau_1} d\tau_2 \Omega_\Theta(z_1,t-\tau_1-\tau_2) \times e^{-\gamma(\tau_1+\tau_2)} j_1(b_2\tau_2) j_1(b_3\tau_1). \tag{36}$$

Just after t_p ($t = t_p + 0$), the functions $B(t)$, $C(t)$, and $D(t)$ are zero. Therefore the amplitude of the output field at $t = t_p$ takes the value

$$\Omega_3(z_3,t_p) = -2\Omega_0 + 2\Omega_\Theta(z_1,t_p) - 2\Omega_\Theta(z_2,t_p) + \Omega_\Theta(z_3,t_p). \tag{37}$$

If $\gamma t_p \ll 1$, then according to the approximate equation (16) this amplitude is approximated as

$$\Omega_3(z_3,t_p) = \Omega_0\{-2 + e^{-\gamma t_p}[2J_0(2\sqrt{b_1 t_p}) - 2J_0(2\sqrt{(b_1+b_2)t_p}) + J_0(2\sqrt{(b_1+b_2+b_3)t_p})]\}, \tag{38}$$

and for the specified values of the parameters b_1, b_2, and b_3 the amplitude of the output field from the composite absorber is 3.65 times larger than the amplitude of the input field Ω_0, and its intensity is 13.36 times larger than the intensity of the incident field. Thus, by the phase shift of the incident fields at the inputs of the layers of the composite absorber we transform the subradiant state of the atom-field system to a superradiant state, which is realized in emission of a short and strong pulse. The shape of the pulse is shown in Fig. 4 for different values of the decay rate of the atomic coherence. The dependence of the normalized maximum of the pulse intensity I_n, induced by the phase shifts, on the number of slices n is shown in the inset of Fig. 4(a) for the case $\gamma t_p \ll 1$.

VI. DISCUSSION

Recently the idea of the transformation of a subradiant state to a superradiant state was experimentally verified

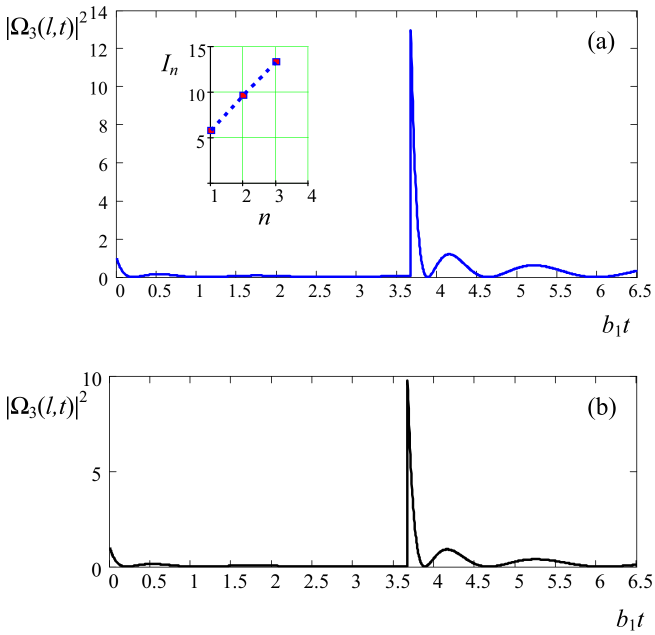

FIG. 4. (Color online) The field intensity at the output of the composite absorber consisting of three slices. The π-phase shift of the fields at the input of all slices of the composite absorber are applied at time t_p satisfying the condition $b_1 t_p = 3.67$, where b_1 is the superradiant rate of the first slice. The time scale is normalized to this rate. The field intensity is normalized to $|\Omega_0|^2$. The decay rates of the atomic coherence are $\gamma = 0.01 b_1$ (a) and $\gamma = 0.1 b_1$ (b). The dependence of the normalized maximum of the pulse intensity I_n, induced by the phase shifts, on the number of slices n is shown in the inset to (a) for the case $\gamma t_p \ll 1$.

with γ-quanta propagating in the sandwich absorbers [15]. Mechanical displacement of odd slices of the composite absorber (sandwich) by a half-wavelength of the radiation field allowed the nuclear coherence along all slices to phase. Since the wavelength of γ-quanta (86 pm for 14.4-keV photons) is extremely small, such a displacement was easily implemented by a polyvinylidene-fluoride (PVDF) piezopolymer thin film. In the optical domain this method is inapplicable, since the radiation wavelength is 3 orders of magnitude larger. Therefore, in this paper different method of effective phasing of the atomic coherence along the composite absorber is proposed. In spite of this difference, comparison of Eq. (32) with Eq. (45) in Ref. [15] shows some similarity of the results. However, there is a qualitative difference in propagation of the step pulse and exponentially decaying pulse through a thick resonant medium if the decay rate of the latter is comparable with the decay rate of the atomic coherence.

It is also interesting to notice that the pulses, produced by the effective phasing of the atomic coherence, look similar to the pulses, generated by stacking of coherent transients [10,11,16,17]. Physically they are different, since the stacking is produced by many pulses or phase switchings at different moments of time. However, the value of the maximum amplitude of the pulse, generated, for example, by two phase switchings,

$$\Omega_{\max}(t_2) = \Omega_0\{2 - 2e^{-\gamma t_1} J_0(2\sqrt{bt_1}) + e^{-\gamma t_2} J_0(2\sqrt{bt_2})\}, \quad (39)$$

almost coincides with the maximum amplitude [Eq. (30)] generated from the composite absorber consisting of two slices if $\gamma t_1 \ll 1$ and $\gamma t_2 \ll 1$. The first term in Eq. (38) corresponds to the transients induced by the second phase switching; the second term describes transients induced by the first phase switching, and the last term describes the transients induced by the leading edge of the step pulse. Here b is the superradiant rate of a single absorber, t_1 is a time interval between the first phase switching and the pulse generation, and t_2 is a time interval between the beginning of the step pulse and the second phase switching. These intervals are chosen such that the functions $J_0(2\sqrt{bt_{1,2}})$ have local extrema. If many phase switchings of the field are applied at particular moments of time, then, as estimated in Refs. [10,11], the maximum intensity of the pulse is 156 times larger than the intensity of the incident field. This is also applicable to the multilayered absorber with a particular combination of thicknesses of the layers.

VII. THE PRACTICALITY OF THE SCHEME WITH THE SLICED ABSORBER

To implement experimentally the proposed scheme with the sliced absorber, one needs an absorbing medium with large optical thickness and a narrow absorption line. It is informative to compare the conditions of phasing of the atomic coherence in the sliced absorber with the conditions for the observation of the stacking of coherent transients in a single absorber. The first experimental observation of the stacking of coherent transients was performed in a gas sample ($HC^{15}N$) with a single absorption line at millimeter wavelength with a width of 100 kHz [11]. Recently, stacking was also observed in the optical domain in cold ^{85}Rb atoms [17]. We can analyze the conditions of generating the superradiant pulse in such a cold gas with homogeneous linewidth $\gamma = 3$ MHz, which corresponds to the dephasing time $T_2 = 53$ ns. To realize the scheme with three slices, we need to satisfy the condition $b_l t_p = 25.87$ at time t_p when the phases of the fields at the entrance of the slices are abruptly changed by π according to Fig. 1. Here, $b_l = b_1 + b_2 + b_3$ is the superradiant rate of the absorber consisting of three slices (see Sec. V).

A. The choice of optical thickness

If we take $\alpha l = 33$ (as in Ref. [17]) for our composite absorber, then $t_p = 83$ ns, which is comparable with $T_2 = 53$ ns. In this case, only 20% of the amplitude of the transients, induced by the appropriate phasing of the absorber slices, contribute, since, for example, for the absorber consisting of two slices the factor of the last two terms in Eq. (30), describing the maximum amplitude of the transients, is $\exp(-t_p/T_2) = 0.2$. Thus, if $\alpha l = 33$, then it is more effective to work with a single sample, since about 80% of gain in the composite absorber is lost due to irreversible dephasing.

Since the equations for the sliced absorber (30) and for the stacking of coherent transients (39) are quite similar, this problem with absorber of effective thickness $\alpha l = 33$ is also relevant to the experiment reported in Ref. [17], where the observed transients were not too large.

If we take $\alpha l = 150$, then time t_p, satisfying the relation $b_l t_p = 25.87$, appreciably shortens to the value $t_p = 18.3$ ns, which is much shorter than $T_2 = 53$ ns. In this case the lengths of the slices satisfy the relations $\alpha l_1 = 21.3$, $\alpha l_2 = 50$, and $\alpha l_3 = 78.7$, and their superradiant times are $T_{R1} = 1/b_1 = 4.986$ ns, $T_{R2} = 1/b_2 = 2.121$ ns, and $T_{R3} = 1/b_3 = 1.349$ ns, respectively. The accuracy in preparation of slices with a given length is not crucial. For example, 10% misfit in the slice lengths with respect to those listed above reduces the intensity of the superradiant pulse only by 7.5%. This is because the maxima of the Bessel functions, which contribute to the amplitude of the signal [see, for example, Eq. (30)], are quite smooth functions of b_n, where $n = 1,2,3$.

B. Arrangement of the absorbing slices

It is possible to place the absorbing slices in a row with large gaps between them, where the phase shifters are placed. As it was already mentioned above, these gaps do not affect the evolution of the field and atomic polarization in the slices. The distance between slices is to be taken into account only for proper synchronization of the phase shifts of the fields at time t_p at the entrance into each slice. For example, for the third slice this time is to be corrected to $t_{p3} = t_p + z_{3\text{in}}/c$, where $z_{3\text{in}}$ is the distance between the front of the first slice and the front of the third slice. If the longitudinal sizes of slices and gaps are large enough, the retardation $z_{3\text{in}}/c$ could be appreciable with respect to the time scale of the superradiant pulse formation.

C. Rate of the phase shift

The subradiant time $T_R = 1/b_l$ of the composite absorber with $\alpha l = 150$ is $T_R = 0.7$ ns. This time defines the rate of the development of the coherently scattered field, which produces the main part of the superradiant pulse after the phase shift of the incident field. Since this time is quite short, the phase shift must be fast. Otherwise, the coherently scattered field will quickly follow any slow change of the field phase and no pronounced transients will be observed after the phase switch. A low-cost waveform generator with 3-ns rise time, used in Ref. [17] for the step phase modulation, is too slow for our scheme. Phase switching time should be at least no longer than 50 ps. Phase shifters with a switch time of 50 ps are practically available (see, for example, Refs. [18,19]). To describe how the phase-shift rate influences the signal, we model the phase shift by the function

$$\varphi(t - t_p) = \tan^{-1}\left(\frac{t - t_p}{\tau_{ph}}\right) + \frac{\pi}{2}, \tag{40}$$

where τ_{ph} is a free parameter. We select such a value of τ_{ph} that in a time interval 50 ps the phase $\varphi(t - t_p)$ changes from 0.1π to 0.9π (see Fig. 5) and find that $\tau_{ph} = 8$ ps.

D. Calculation of the signal at the exit of the slices

If the phase of the field incident to the composite absorber changes at time t_p in accordance with Eq. (40), then the field at the exit of the first slice of the absorber is

$$\Omega_{\varphi 1}(z_1,t) = \Omega_0\Theta(t)\left[e^{i\varphi_1(t)} - b_1\int_0^t e^{i\varphi_1(t-\tau)-\gamma\tau} j_1(b_1\tau)d\tau\right], \tag{41}$$

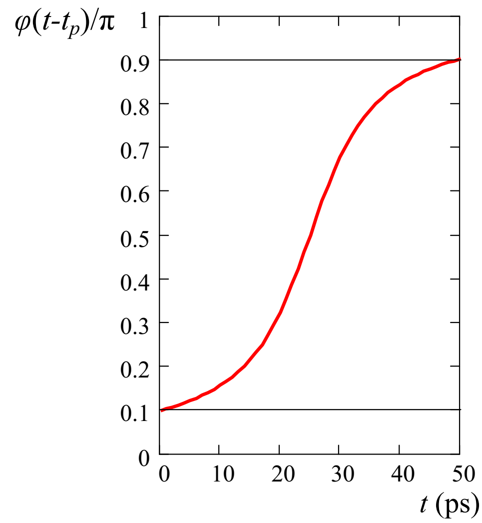

FIG. 5. (Color online) Time dependence of the phase variation in time (bold solid line). The parameters are $\tau_{ph} = 8$ ps and $t_p = 25$ ps. Thin horizontal lines show the borders of the phase change within the time interval 50 ps.

where $\varphi_1(t) = \varphi(t - t_p)$. Below we adopt the values of the relevant parameters as $T_2 = 53$ ns, $t_p = 18.3$ ns, $T_{R1} = 1/b_1 = 4.986$ ns, and $\tau_{ph} = 8$ ps. Time dependence of this field intensity is compared with that for the field, produced by the instantaneous phase shift by π [Eq. (23)] in Fig. 6(a), where only a short time window, demonstrating the formation of the superradiant pulse, is shown. Due to the noninstantaneous phase shift, the maximum of the pulse intensity decreases only by 2.5%.

A phase shift of the field at the entrance of the second slice, $\varphi_2(t) = \varphi(t - t_p)$, results in

$$\Omega_{\varphi 1}(z_1,t)e^{i\varphi_2(t)}. \tag{42}$$

This field is transformed to

$$\Omega_{\varphi 2}(z_2,t) = e^{i\varphi_2(t)}\Omega_{\varphi 1}(z_1,t) - b_2\int_0^t e^{i\varphi_2(t-\tau)-\gamma\tau} \times \Omega_{\varphi 1}(z_1,t-t_p)j_1(b_2\tau)d\tau \tag{43}$$

at the exit of the second slice. Time dependence of the field intensity is compared in Fig. 6(b) with that for the field generated at the exit of the second slice if instantaneous phase shifts of the fields by π take place simultaneously at time t_p before the entrances of the first and second slices of the composite absorber [Eq. (27)]. The superradiant time of the second slice is $T_{R2} = 1/b_2 = 2.121$ ns. The maximum intensity of the superradiant pulse decreases by 5% due to noninstantaneous phase shift of the fields entering the slices.

Phase shift, $\varphi_3(t) = \varphi(t - t_p)$, of the field at the entrance of the third slice,

$$\Omega_{\varphi 2}(z_2,t)e^{i\varphi_3(t)}, \tag{44}$$

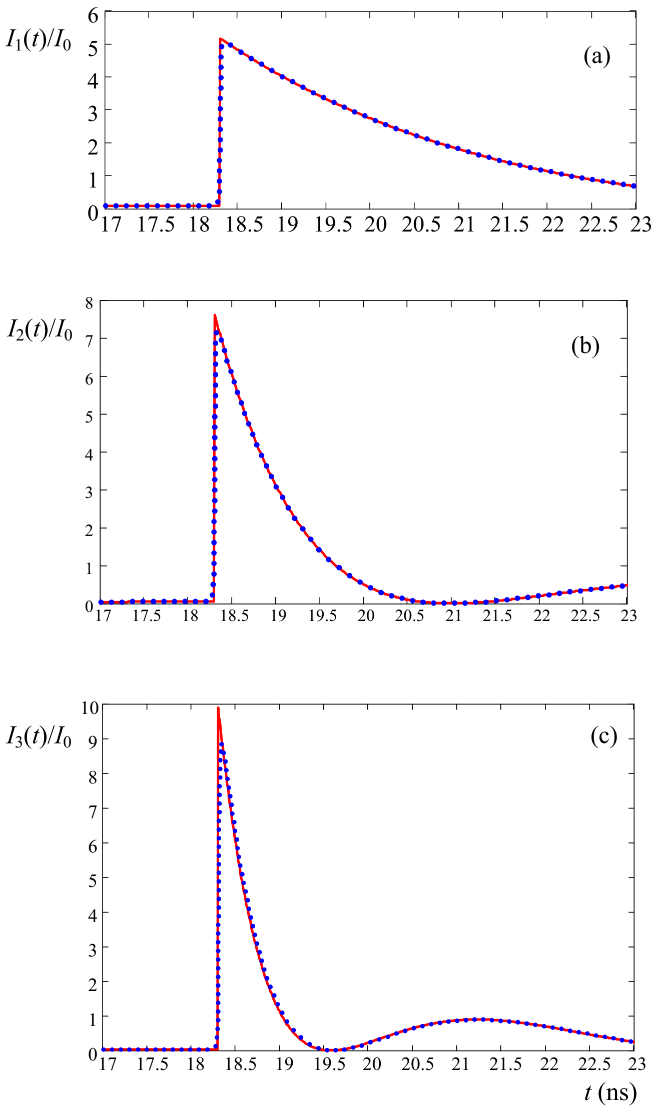

FIG. 6. (Color online) Time dependence of intensity of the field $I_n(t)$ at the exit of the nth slice ($n = 1,2,3$). I_0 is the intensity of the field incident to the composite absorber. The solid line (in red) shows the intensity time dependence for the instantaneous phase shifts. Dots (in blue) show the intensity if the phases change smoothly. Parameters are defined in the text.

results in the following evolution of the field at the exit of the composite absorber:

$$\Omega_{\varphi 3}(z_3,t) = e^{i\varphi_3(t)}\Omega_{\varphi 2}(z_1,t) - b_3 \int_0^t e^{i\varphi_3(t-\tau)-\gamma\tau} \times \Omega_{\varphi 2}(z_1,t-t_p) j_1(b_3\tau) d\tau. \quad (45)$$

Comparison of intensity of this field with the intensity of the field generated by the instantaneous phase shifts [Eq. (32)] is shown in Fig. 6(c), which demonstrates that the noninstantaneous character of the phase shifts decreases the intensity of the superradiant pulse by 10%.

E. Nonsimultaneous phase shifts

Below we analyze the case if the phases of the fields in front of the slices are switched not simultaneously, for example, because of bad synchronization of the phase shifters. For simplicity, our consideration is limited by the absorber consisting of two slices with effective superradiant rates b_1 and b_2. We assume that the phase shifts $\varphi_1(t)$ and $\varphi_2(t)$ take place at times $t_p = t_1$ and $t_p = t_2$, respectively. Then the output field from the composite absorber is described by Eq. (43). For the stepwise phase shifts this equation is reduced to

$$\Omega_2(z_2,t) = \Omega_\Theta(z_2,t) - 2\{\Omega_\Theta(z_2,t-t_1) + \Theta(t-t_2)[\Omega_{12}(z_1,z_2,t,t_2) - 2\Omega_{12}(z_1,z_2,t-t_1,t_2-t_1)]\} \quad (46)$$

if $t_2 > t_1$, and

$$\Omega_2(z_2,t) = \Omega_\Theta(z_2,t) + 2[\Omega_\Theta(z_2,t-t_1) - \Theta(t-t_2) \times \Omega_{12}(z_1,z_2,t,t_2)] \quad (47)$$

if $t_1 > t_2$.

In both cases two distinguished pulses appear at $t = t_1$ and $t = t_2$. The absolute value of the amplitude of the first pulse is smaller than that of the second pulse. If $t_2 > t_1$ and $\gamma t_{1,2} \ll 1$, then the amplitudes of the pulses are

$$\Omega_2(z_2,t_1) = \Omega_0[J_0(2\sqrt{(b_1+b_2)t_1}) - 2], \quad (48)$$

$$\Omega_2(z_2,t_2) = \Omega_0\{J_0(2\sqrt{(b_1+b_2)t_2}) - 2[J_0(2\sqrt{(b_1+b_2)(t_2-t_1)}) + J_0(2\sqrt{b_1 t_2}) - 2J_0(2\sqrt{b_1(t_2-t_1)})]\}. \quad (49)$$

If $t_1 > t_2$ and $\gamma t_{1,2} \ll 1$, then

$$\Omega_2(z_2,t_2) = \Omega_0[J_0(2\sqrt{(b_1+b_2)t_2}) - 2J_0(2\sqrt{b_1 t_2})], \quad (50)$$

$$\Omega_2(z_2,t_1) = \Omega_\Theta(z_2,t_1) + 2[\Omega_\Theta(z_2,0) - \Omega_{12}(z_1,z_2,t_1,t_2)]. \quad (51)$$

Figure 7 shows the dependence of the intensity of the second pulse on the time difference $t_2 - t_1$ if $T_{R1} = 1/b_1 = 4.986$ ns, $T_{R2} = 1/b_2 = 2.121$ ns, $t_1 = 18.3$ ns, $T_2 \to \infty$, and the phases are switched instantaneously. For the given values of the parameters, the second pulse has maximum if $t_2 - t_1 =$

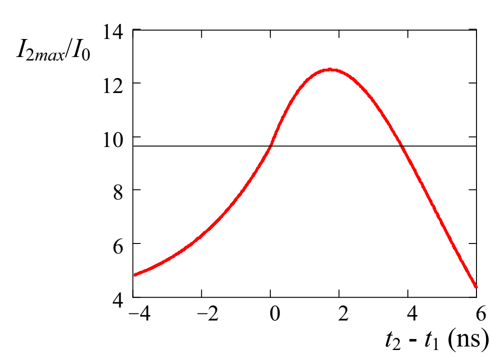

FIG. 7. (Color online) Normalized maximum intensity of the second superradiant pulse $I_{2\max}$ versus $t_2 - t_1$, bold solid line. Thin horizontal line shows maximum intensity for $t_2 = t_1$.

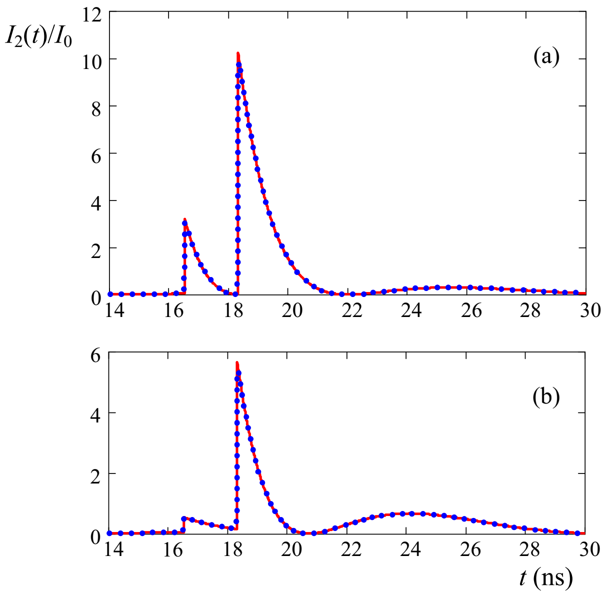

FIG. 8. (Color online) Time dependence of the pulses induced by nonsimultaneous phase shifts of the fields in front of two slices of the composite absorber. The solid line (in red) corresponds to the instantaneous phase shifts and the dotted line (in blue) corresponds to the case of smooth phase shifts (during 50 ps). The time delay between phase shifts is 1.8 ns. The moments of time of the phase shifts are $t_1 = 16.5$ ns, $t_2 = 18.3$ ns in (a), and $t_1 = 18.3$ ns, $t_2 = 16.5$ ns in (b).

1.8 ns. Its intensity increases by 30% with respect to the intensity of the pulse when $t_2 = t_1$. We assume that two effects, i.e., phasing of the atomic coherence and stacking of the coherent transients, together give the intensity enhancement of the superradiant pulse. Figure 8 shows these pulses if the coherence decay $T_2 = 53$ ns and noninstantaneous phase shifts with parameter $\tau_{ph} = 8$ ps are taken into account.

F. The switching time of the field

We considered the excitation of the composite absorber by the step pulse, which is switched on instantly at time $t = 0$. This is also an idealization. Let us suppose that the input pulse is switched on slowly according to the expression

$$\Omega(0,t) = \Omega_0\Theta(t)(1 - e^{-t/\tau_{\rm on}}), \tag{52}$$

where time $\tau_{\rm on}$ is the rise time of the field amplitude. Then, for example, at the exit of the first slice this field is transformed to

$$\Omega(z_1,t) = \Omega_0\Theta(t)\gamma \int_0^t \left[1 + \left(\frac{1-\gamma\tau_{\rm on}}{\gamma\tau_{\rm on}}\right) e^{-(t-\tau)/\tau_{\rm on}}\right] \times e^{-\gamma\tau} J_0(2\sqrt{b_1\tau})d\tau. \tag{53}$$

If, for example, the amplitude of the incident field [Eq. (52)] reaches 90% of its maximum value within 3 ns, then $\tau_{\rm on} = 1.3$ ns. Comparison of $\Omega(z_1,t)$ [Eq. (53)] with the output field amplitude $\Omega_\Theta(z_1,t)$, produced by the step pulse incident to the first slice ($T_{R1} = 1/b_1 = 4.986$ ns, $T_2 = 52$ ns), is shown in Fig. 9. It is seen that the front parts of these fields are different, while the following wiggles approach each other very fast. For this reason, we expect that the way of switching on the incident pulse is not so important for the process of coherence phasing if $\tau_{\rm on} \ll T_{R1}$. In real experiments it is preferable to use the cw incident field with fast switching of its phase at $t = 0$ instead of stepwise switching of the incident field at $t = 0$.

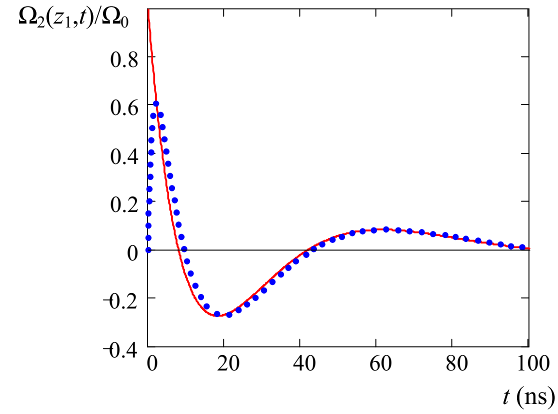

FIG. 9. (Color online) Time dependence of the fields at the exit of the first slice. They are produced by the input step pulse (solid line in red) and pulse whose front grows slowly according to Eq. (52) (dots in blue). Details are in the text.

VIII. CONCLUSION

In this paper it is shown that during the step pulse propagation through a thick resonant absorber, the atomic coherence is formed into spatial domains with opposite phases. As a result, a subradiant state is developed in the absorber. It is proposed to divide the absorber into slices in accordance with these domains and place phase shifters between them and in front of the absorber. Fast phase switching of the incident fields at the input of each slice transforms the subradiant state to a superradiant state, seen as a strong and short pulse. The intensity of the produced pulse is an order of magnitude larger with respect to the intensity of the incident field, while in CRIB and echo techniques the pulses produced are smaller.

ACKNOWLEDGMENTS

Partial support by the National Science Foundation (Grant No. PHY-1307346), the Russian Foundation for Basic Research (Grant No. 12-02-00263-a), the Program of Competitive Growth of Kazan Federal University funded by the Russian Government, and the RAS Presidium Program "Quantum Mesoscopic and Disordered Systems" is acknowledged.

APPENDIX

To calculate the output field from the second slice of the absorber if the input field is $\Omega_\Theta(z_1,t)$ or $\Omega_\Theta(z_1,t-t_p)$, we use Eq. (9), which is reduced, for example, for $\Omega_\Theta(z_1,t)$ to the expression

$$\Omega_\Theta(z_2,t) = \Omega_\Theta(z_1,t) - \int_0^t \Omega_\Theta(z_1,t-\tau) \times e^{-\gamma\tau}\sqrt{\frac{b_2}{\tau}}J_1(2\sqrt{b_2\tau})d\tau. \tag{A1}$$

Then we apply the Laplace transform

$$F(p) = \int_0^{+\infty} e^{-pt} f(t) dt \tag{A2}$$

to the function $\Omega_\Theta(z_2,t)$. It can be done in the following way. First we calculate the Laplace transform of the function $\Omega_\Theta(z_1,t)$ in the form represented in Eq. (12). The Laplace transform of the function $\sqrt{b_1/t}\,J_1\left(2\sqrt{b_1 t}\right)$ in the integral term in Eq. (12) can be found with the help of the differentiation theorem. This Laplace transform is

$$1 - e^{-b_1/p}. \tag{A3}$$

Then the Laplace transform of the whole integral term in Eq. (12) can be calculated with the help of the linear transformation and integration theorems. The result of this calculation is

$$\frac{1}{p}[1 - e^{-b_1/(p+\gamma)}]. \tag{A4}$$

Finally, the Laplace transform of $\Omega_\Theta(z_1,t)$ is

$$\Omega_\Theta(z_1,p) = \frac{1}{p} e^{-b_1/(p+\gamma)}. \tag{A5}$$

Second, since the integral in Eq. (A1) is the convolution of two functions, the Laplace transform of the right-hand side of Eq. (A1) is

$$\Omega_\Theta(z_1,p) - \Omega_\Theta(z_1,p)(1 - e^{-b_2/(p+\gamma)}). \tag{A6}$$

Combining Eqs. (A5) and (A6), we obtain the Laplace transform of $\Omega_\Theta(z_2,t)$, which is

$$\Omega_\Theta(z_2,p) = \frac{1}{p} e^{-(b_1+b_2)/(p+\gamma)}. \tag{A7}$$

Comparison of Eq. (A7) with Eq. (A5) gives the result that transmission of the field $\Omega_\Theta(z_1,t)$ through the second slice of length $l - z_1$ simply changes the argument z_1 of the function describing the field to $z_2 = l$. This result is obvious, since without phase shifters the light propagation through two slices, having effective thickness parameters b_1 and b_2 and placed in a row, is the same as the light propagation through the absorber with the effective thickness parameter $b_l = b_1 + b_2$.

[1] M. D. Crisp, Phys. Rev. A **1**, 1604 (1970).

[2] K. E. Oughstun, *Electromagnetic and Optical Pulse Propagation 2: Temporal Pulse Dynamics in Dispersive Attenuative Media* (Springer, New York, 2009).

[3] E. Yablonovitch, Phys. Rev. A **10**, 1888 (1974).

[4] A. A. Kalachev and V. V. Samartsev, Kvantovaya Elektron. (Moscow) **35**, 679 (2005); Quantum Electron. **35**, 679 (2005).

[5] A. Kalachev and S. Kroll, Phys. Rev. A **74**, 023814 (2006).

[6] A. Kalachev, Phys. Rev. A **76**, 043812 (2007).

[7] A. Kalachev and S. Kroll, Phys. Rev. A **78**, 043808 (2008).

[8] A. Walther, A. Amari, S. Kroll, and A. Kalachev, Phys. Rev. A **80**, 012317 (2009).

[9] E. Varoquaux, G. A. Williams, and O. Avenel, Phys. Rev. B **34**, 7617 (1986).

[10] B. Macke, J. Zemmouri, and B. Segard, Opt. Commun. **59**, 317 (1986).

[11] B. Segard, J. Zemmouri, and B. Macke, Europhys. Lett. **4**, 47 (1987).

[12] D. C. Burnham and R. Y. Chao, Phys. Rev. **188**, 667 (1969).

[13] R. N. Shakhmuratov, Phys. Rev. A **85**, 023827 (2012).

[14] R. P. Feynman, R. B. Leighton, and M. Sands, *The Feynman Lectures on Physics*, Vol. I (Addison-Wesley, Reading, MA, 1963).

[15] R. N. Shakhmuratov, F. Vagizov, and O. Kocharovskaya, Phys. Rev. A **87**, 013807 (2013).

[16] H. Jeong and S. Du, Opt. Lett. **35**, 124 (2010).

[17] J. F. Chen, H. Jeong, L. Feng, M. M. T. Loy, G. K. L. Wong, and S. Du, Phys. Rev. Lett. **104**, 223602 (2010).

[18] A. Z. Genack and R. G. Brewer, Phys. Rev. A **17**, 1463 (1978).

[19] A. Z. Genack, D. A. Weitz, R. M. Macfarlane, R. M. Shelby, and A. Schenzle, Phys. Rev. Lett. **45**, 438 (1980).